Theoret. Chim. Acta (Berl.) 47, 315–328 (1978)

THEORETICA CHIMICA ACTA

INDO Calculations with Inclusion of an Effective Solvent Field. Application to Benzosemiquinones

Jens Spanget-Larsen

Institut für Organische Chemie der Technischen Hochschule Darmstadt, Petersenstrasse 22, D-6100 Darmstadt, Federal Republic of Germany

An INDO method extended to include a contribution from the solvent by means of an effective solvent field (ESF) is applied to the three isomeric benzosemiquinones and some of their alkyl derivatives. The calculations lead to a satisfactory description of the hyperfine coupling constants, in contrast to traditional calculations. The results imply that the spin distribution in *p*- and *o*-semiquinones is largely determined by the influence of the solvent; in particular, the influence is able to invert the order of the spin densities at the 3 and 4 positions in 1,2-benzosemiquinone.

Key words: INDO method with a contribution from the solvent – Benzosemiquinones, spin densities and geometries of ~

1. Introduction

Since the introduction by Pople and coworkers [1], the INDO method has been widely used in the calculation of hyperfine coupling constants of radicals [1, 2]. Numerous successful applications have been published, but at least one class of radicals remains for which the standard INDO method yields poor results, namely the semiquinone radical anions [1]. This is unfortunate, e.g. because naturally occurring quinones and hydroquinones are often characterized through the ESR spectra of the corresponding semiquinones [3]. The discrepancy is a general phenomenon, i.e. semiempirical procedures which reproduce the hyperfine constants of *p*-semiquinones do not apply to *o*-semiquinones [4, 5]. It has recently been suggested that the reason for this situation is the strong interaction between the radicals and the solvent [6, 7]. In order further to investigate this problem, an INDO method extended to include a simple electrostatic contribution from the solvent is applied in this paper to the three isomeric benzosemiquinones **1**, **2** and **3** and the alkyl derivatives **1a**, **1b**, **2a** and **2b**.

0040–5744/78/0047/0315/$02.80

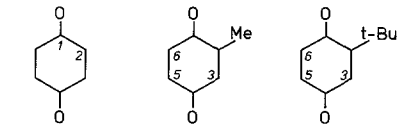

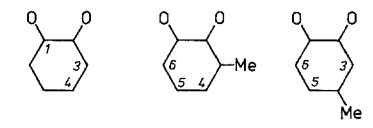

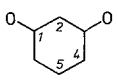

2. The Effective Solvent Field (ESF) Model

The solvation of molecules in solution is a matter of fundamental importance in chemistry and biology. The theoretical treatment of the liquid phase, however, is more difficult than the treatment of the gas phase or the solid phase, and calculations of solvent effects are usually quite approximate [8]. The classical electrostatic solvation model is based on the assumption that the interaction between solvent and solute species can be represented by purely Coulombic forces [8, 9]. In the present investigation it will be assumed that the orientation of the permanent dipoles of the solvent species and the rapidly changing formation and breaking of complexes between solute and solvent can be considered as giving rise to an effective solvent field (ESF) at the position of the solute species [10, 11]. Particularly important is the possible gradient of the ESF which may lead to electron reorganization in the solute molecule.

The ESF can be approximated by the field from a number of point charges. In a study of the solvent sensitivities of the hyperfine coupling constants of the nitrobenzene radical anion it was found that an INDO calculation including the field from a single external point charge gave a very satisfactory agreement with the experimental data [10]. A simple way to represent an external point charge in the INDO computer program is by means of a pseudo proton with its $1s$ orbital prevented from being occupied; this is achieved by assigning to the core energy an "infinitely large" value. The core charge of this pseudo proton is then treated as an input parameter, q, which may be positive or negative [10, 11]. In this way only minor modifications of the available computer program [1, 12] are required. The field of this point charge is not a pure Coulombic field because the two-center core-electron interaction terms in the INDO approximation are set equal to the corresponding electron repulsion integrals with negative sign (neglect of penetra-

tion) [1]. However, this screening of the potential is not significant to the performance of the simple model.

The basic concept of an ESF is very simple, and the point charge approximation could easily turn out to be an oversimplification. It will be shown in this paper, however, that the model is adequate for the strongly solvated semiquinone radical anions. The INDO results described in the following were obtained with the inclusion of the field from two external positive point charges q, one per oxygen atom in the radical. The point charges were positioned on the C–O axes with $q\cdots$O distances equal to 1.5 Å. This arrangement reflects the tendency to solvate the highly charged oxygen atoms [13]. Previous investigations [6, 7] indicate that the bulk of the methyl group in **1a**, **2a** and **2b** does not significantly hinder the solvation by water. In the case of **1b**, however, it must be assumed that the bulky *t*-butyl group introduces considerable asymmetry into the solvation [6]. The point charge model for **1b** is modified accordingly: the position of the point charge at the

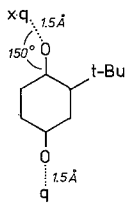

oxygen flanked by the *t*-butyl group is taken to form a $q\cdots$O–C angle of 150°, as indicated above; this position is approximately intermediate between the *t*-butyl group and the ring hydrogen at position 6 (see later). The point charge at the hindered position is furthermore taken to be less than the point charge at the unhindered position by a factor x. The appropriate value of this asymmetry parameter is determined by comparison with experiment.

The calculations were carried out as described previously [10]. In the INDO approximation the isotropic hyperfine coupling constant a_X of a nucleus X is proportional to the spin population ρ_{ns} of the valence s atomic orbital (AO) of the atom X [1]. In the present investigation, the calculated results will be discussed in terms of the predicted s-type spin densities ρ_{ns}, mainly because the proportionality factor relating proton coupling constant to H1s spin density in the original INDO parametrization [1] is not adequate for semiquinones [1, 11, 14]. As a calculated measure of the solvent sensitivity of the spin population ρ_{ns} is defined the derivative $\rho'_{ns}=\partial\rho_{ns}/\partial q$. The appropriate value of q for a given solvent is derived by comparison with the observed coupling constants a_X and their solvent sensitivities a'_X. It is found that the order of magnitude of q is 1e (e = elementary charge $\approx 1.6022\times10^{-19}$ C).

3. Optimization of Geometry

Calculated spin densities are known to be sensitive to the choice of molecular geometry [15]. It is thus important to obtain a reasonable estimate of the structure

of the radicals. In the present study the geometry of **1**, **2** and **3** has been calculated by the MINDO/3-UHF method [15]. The symmetry was assumed to be D_{2h} in the case of **1** and C_{2v} in the case of **2** and **3**. The results are shown in Fig. 1. The calculated geometry of **1** may be compared with the one calculated for 1,4-benzoquinone [16]; the carbonyl bond is longer and the bond alternance, although still appreciable, is much less pronounced in the case of **1**. This is consistent with the usual representation of the radical as an aromatic species.

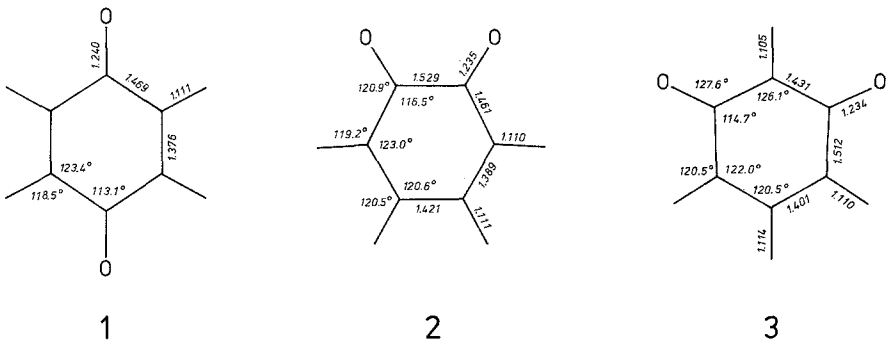

Fig. 1. Geometries of the semiquinone radicals **1**, **2** and **3** calculated by the MINDO/3-UHF method

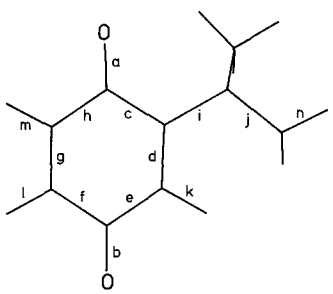

Fig. 2. Calculated geometry of **1b**.
Distances (Å):
$a=1.235$, $b=1.239$, $c=1.500$, $d=1.408$, $e=1.459$, $f=1.470$, $g=1.362$, $h=1.472$, $i=1.592$, $j=1.544$, $k=1.110$, $l=1.110$, $m=1.111$, $n=1.112$.
Angles:
$ac=123.4°$, $cd=118.5°$, $de=126.4°$, $ef=113.2°$, $fg=122.8°$, $gh=124.5°$, $be=123.5°$, $ci=119.4°$, $ij=112.2°$, $dk=116.0°$, $gl=119.6°$, $gm=117.1°$, $jn=114.6°$

The structure of the methyl derivatives **1a**, **2a** and **2b** was derived from the calculated geometry for **1** and **2**. The C–C and C–H distances of the substituted methyl group were taken as 1.5 Å and 1.1 Å, respectively; the CCH and HCH angles were taken as tetrahedral and the C–C axis was chosen to coincide with the C–H axis of the parent compound. Variation of these geometrical parameters was found to affect insignificantly the trends of the calculated spin distributions.

The bulk of a *t*-butyl substituent can be expected to have a larger impact on the structure than that of a methyl substituent. Fairbourn and Lucken [17] have suggested that the steric effect of the *t*-butyl group may lead to compression of the neighbouring carbonyl group in **1b**. In order to check this hypothesis the geometry of **1b** has been calculated by MINDO/3-UHF. The results are given in Fig. 2. **1b** was assumed to contain a plane of symmetry, and the orientation of the alkyl group was taken as indicated in Fig. 2. The *t*-butyl group and each of the three

methyl groups were assumed to possess local C_{3v} symmetry. This assumption is not totally unreasonable since *t*-butyl groups in semiquinones are known to rotate freely with all nine protons being equivalent [18]. The results in Fig. 2 indicate that the compression of the carbonyl bond is negligible; the distortion of the ring is significant, however.

The calculated structures discussed above do not include the possible influence of the solvent. Solvation of the carbonyl group can thus be expected to lengthen the C–O distance. To get some sort of an estimate of this effect the geometry of monoprotonated **2** has been optimized by MINDO/3-UHF within C_{2v} symmetry. The resulting O···H distances are 1.238 Å, similar to the value obtained by a recent INDO calculation [19]. The lengthening of the C–O distances is predicted to be less than 0.04 Å, which is not essential to the calculated spin distribution. On the whole, the predicted distortion of the geometry of **2** by the monoprotonation (within C_{2v}) is minor. The structures given in Figs. 1 and 2 are thus assumed to be sufficiently adequate for the solvated species.

The influence of the geometry optimization on the calculated spin densities is significant; e.g. in the case of **2** the INDO calculation ($q=0$) based on the optimized geometry predicts negative spin density on the hydrogen atoms at the 4 and 5 positions, in contrast to the result obtained on the basis of a regular geometry [1, 20]. With regard to agreement with experiment, however, the use of optimized structures alone does not prevent discrepancy, see below.

4. Results and Discussion

4.1. The 1,4-Benzosemiquinones **1**, **1a** *and* **1b**

The $p\pi$ spin populations of **1** obtained by a standard INDO calculation ($q=0$) are shown schematically in Fig. 3a.

Close to 90% of the spin density is localized on the oxygen atoms. Increasing the ESF leads to redistribution of positive spin density from the oxygen atoms to the ring, particularly to the carbonyl carbon positions, see Fig. 3b. The influence on the remaining ring positions is small; this is partly due to the high symmetry of the

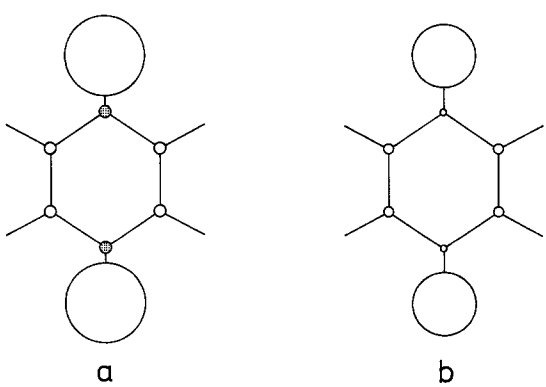

Fig. 3. Calculated π spin populations of **1**. The diameters of the circles indicate the relative spin populations, shading indicates negative spin density. (*a*) $q=0$, (*b*) $q=0.9$e

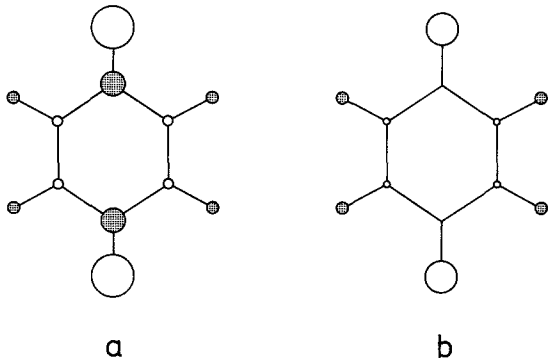

Fig. 4. Calculated 1*s* and 2*s* spin populations of **1**. The diameters of the circles indicate the relative spin populations (the scale is different from Fig. 3), shading indicates negative spin density. (*a*) $q=0$, (*b*) $q=0.9e$

radical which leaves little room for rearrangement of the spin density on these positions. These trends are well known and are easily reproduced by simple solvation models [6, 21, 22]. Similar trends are shown to an even more striking degree by the calculated *s* AO spin populations, see Fig. 4. The influence of the ESF on the *s*-type spin distribution is shown in Fig. 5, where the calculated valence 1*s* and 2*s* spin densities are plotted as a function of q/e.

The predicted solvent sensitivities indicated in Fig. 5 are consistent with the measured solvent dependence of the ^{17}O and ^{13}C hyperfine constants of **1**. The shifts predicted by an increase of ESF in the model correspond to the shifts observed when the solvent is changed from non-polar and aprotic to polar and protic [21, 23, 24]. The solvent sensitivity of the ^{13}C coupling constant in position 1 is particularly large. The measured value is -2.13 G in dimethylsulfoxide and $+0.24$ G in water [23] (Gauss$=10^{-4}$ Tesla). The change of sign is significant, it indicates that the appropriate ESF corresponds to $q\approx 1e$ (see Figs. 4b and 5).

The calculated spin populations ρ_{1s} and their solvent sensitivities ρ'_{1s}, as well as the measured quantities a_H and a'_H, are included in Table 1. The observed relative solvent sensitivities for **1** and **1a** are well predicted by the calculation, although a

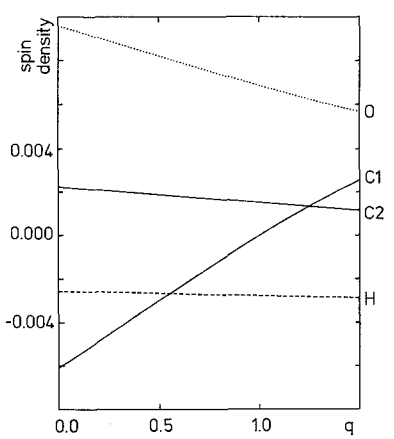

Fig. 5. Calculated 1*s* and 2*s* spin populations of **1** as a function of the ESF

Table 1. Calculated spin populations ρ and their derivatives $\rho' = \partial\rho/\partial q$; observed proton hyperfine coupling constants a_H and their derivatives $a'_H = \partial a_H/\partial X_{H_2O}$, where X_{H_2O} is the molar fraction of water in the solvent mixture

Compound	Position	INDO[a]	INDO-ESF[b]		EWMO-ESF[c]		Observed[c]	
		$10^4 \cdot \rho_{1s}$	$10^4 \cdot \rho_{1s}$	$10^4 \cdot \rho'_{1s}$	$-10^3 \cdot \rho_\pi$	$-10^3 \cdot \rho'_\pi$	a_H	a'_H
1	2	−26	−28	−1	−62	+8	−2.36	+0.06
1a	3	−30	−24	+6	−43	+29	−1.76	+0.16
	5	−27	−32	−5	−77	0	−2.58	+0.02
	6	−22	−24	0	−61	+23	−2.41	+0.13
	Me[d]	+37	+45	+10	----------		+2.08	+0.19
1b	3	−32	−11	+28	−15	+32	−1.65	+0.27
	5	−22	−15	+11	−52	+26	−2.14	+0.20
	6	−25	−39	−19	−78	−8	−2.85	−0.01
2	3	−50	−12	+28	−22	+61	−0.85	+0.80
	4	−13	−35	−20	−64	−56	−3.60	−0.63
2a	4	−17	−30	−14	−46	−32	−2.85	−0.11
	5	−9	−36	−23	−66	−70	−4.04	−0.74
	6	−52	−8	+31	−12	+53	−0.38	+0.86
	Me[d]	+69	+20	−33	----------		+0.68	−0.35
2b	3	−51	−3	+34	−6	+58	−0.22	+0.89
	5	−10	−37	−26	−81	−77	−3.73	−0.41
	6	−54	−15	+30	−27	+53	−1.00	+0.61
	Me[d]	+28	+62	+38	----------		+4.68	+1.36
3	2	−1	−11	−2	----------		−0.63	~0
	4	−210	−215	0	----------		−11.30	~0
	5	+109	+107	−4	----------		+2.40	~0

[a] $q = 0$.
[b] $q = 1.1$e, except for **1b** where $q = 0.7$e.
[c] Refs. [6, 7, 25, 29].
[d] The quoted spin population is an average value for the three methyl hydrogens.

trend towards too negative values is apparent. The relative magnitudes of the proton coupling constants are not well reproduced. This is not essential, the spread of the ring coupling constants is only 0.82 G (0.34 G in hexamethylphosphoramide [14]). The correct ordering can be obtained by manipulation of the geometry [14]. Previous results [6] obtained by the Energy Weighted Maximum Overlap (EWMO) method [26, 27] are slightly better than the INDO results for **1** and **1a**; the EWMO results are included in the table for comparison.

As mentioned in Sect. 2, it is necessary to introduce an asymmetry parameter x in the case of the *t*-butyl derivative **1b**. Three series of calculations were performed with $x = 1$, $x = \frac{3}{4}$ and $x = \frac{1}{2}$. $x = 1$ corresponds to no asymmetry of the solvation and

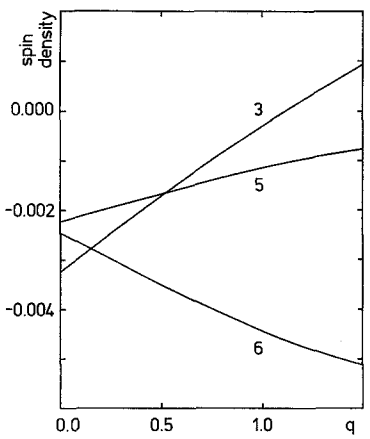

Fig. 6. Calculated ring hydrogen 1*s* spin populations of **1b** as a function of the ESF ($x=\frac{3}{4}$)

is found to yield poor agreement with experiment. The choice $x=\frac{1}{2}$, on the other hand, overestimates the asymmetry; $x=\frac{3}{4}$ appears to be a reasonable compromise. The calculated ring hydrogen spin densities of **1b** for $x=\frac{3}{4}$ are plotted as a function of q in Fig. 6. The corresponding proton couplings are shown as a function of the molar fraction of water, X_{H_2O}, in a H_2O-dimethylformamide solvent mixture [6] in Fig. 7. The calculated results reproduce fairly well the trends observed by an increase of polarity of the medium. The results support the conclusion based on the previous EWMO investigation [6]: the characteristic features of the proton coupling constants of the *t*-butyl derivatives of **1** in polar and protic solvents are due primarily to solvation.

4.2. The 1,2-Benzosemiquinones **2**, **2a** *and* **2b**

The spin distribution of **2** recalls that of **1**; by far the largest part of the predicted spin density is localized on the oxygen atoms, see Fig. 8. Inclusion of the ESF results in displacement of spin density from the oxygen atoms to the ring atoms. The most important trend, however, is the tendency to rearrangement of the spin distribution in the ring as the strength of the ESF is increased. This is evident from Fig. 8, and in particular from Fig. 9, which shows the predicted *s*-type spin distributions. The influence of the ESF is noteworthy. The calculated valence *s* AO spin populations of **2** are shown as a function of q in Fig. 10; it is seen that an ESF corresponding to $q \approx 1e$ leads to almost total rearrangement of the *s*-type spin distribution, reversing the order of the spin populations at the 3 and 4 positions. The order of the H_{1s} spin populations so obtained is in agreement with the order of the measured proton splittings: $a_{H3} > a_{H4}$ [5, 28] (both constants are negative).

Investigation of the monomethyl derivatives **2a** and **2b** provides further data. Calculated and measured results are included in Table 1. A clear trend is realized by consideration of the results for the methyl protons in **2a** and **2b**. The calculation

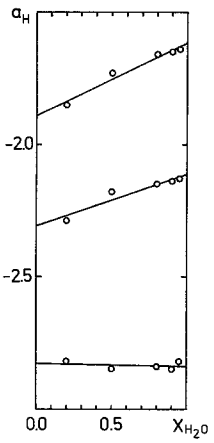

Fig. 7. Measured ring proton couplings a_H(G) of **1b** as a function of the molar fraction of water X_{H_2O} in a H_2O-dimethylformamide solvent mixture [6]

with no ESF predicts a larger spin population of the methyl hydrogens in **2a** than in **2b**; inclusion of the ESF leads to reversal of the predicted order and, in so doing, to agreement with the observed order of the coupling constants (see Table 1). This trend is consistent with the signs of the measured solvent sensitivities, although the predicted sensitivity is too large for **2a** relative to **2b**.

The calculated ring hydrogen spin populations of **2**, **2a** and **2b** are plotted in

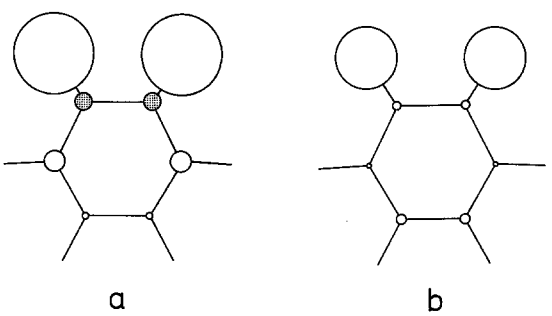

Fig. 8. Calculated π spin populations of **2**. The figure is similar to Fig. 3. (*a*) $q=0$, (*b*) $q=0.9$e

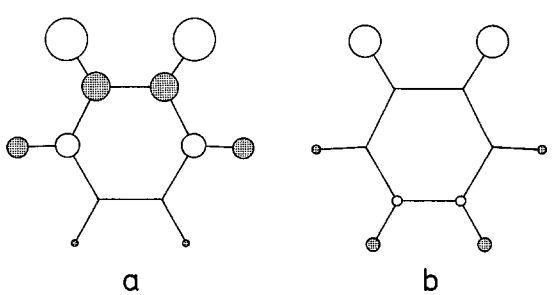

Fig. 9. Calculated 1*s* and 2*s* spin populations of **2**. The figure is similar to Fig. 4. (*a*) $q=0$, (*b*) $q=0.9$e

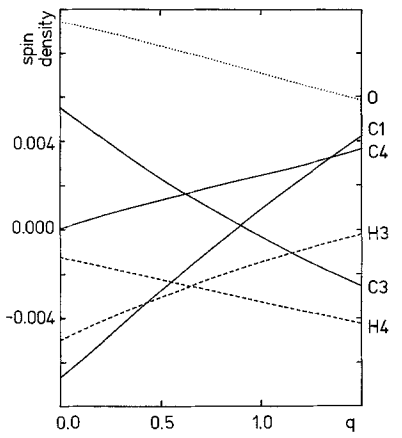

Fig. 10. Calculated 1*s* and 2*s* spin populations of **2** as a function of the ESF

Fig. 11 as a function of q. The corresponding coupling constants are shown in Fig. 12 as a function of the molar fraction of water in a H_2O-dioaxane solvent mixture [7]. The plots show that accordance between calculated and measured results can only be obtained by assumption of a considerable ESF. An ESF corresponding to $q \approx 1e$ leads to good agreement between calculated and observed positions with respect to relative order of magnitude.

The linear regression of the observed proton coupling constants on the calculated spin populations (see Table 1) is shown in Fig. 13. The results for **1** and **1a** are included in the figure and are seen to fit well into the correlation. If all ring and methyl positions in **1**, **1a**, **2**, **2a** and **2b** are considered, the following linear relation is obtained by means of the least squares criterion:

$$a_H = 763\rho_{1s} - 0.42 \tag{1}$$

(a_H in G). The regression coefficient is 0.974 and the standard deviation is 0.52 G. Including only ring positions in the correlation the result is

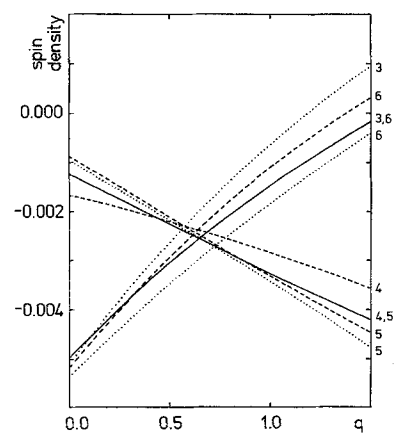

Fig. 11. Calculated ring hydrogen spin populations of **2** (full curves), **2a** (broken curves), and **2b** (dotted curves) as a function of the ESF

$$a_H = 1105\ \rho_{1s} + 0.47 \quad (2)$$

with regression coefficient 0.972 and standard deviation 0.29 G. These results are quite satisfactory; it is evident that the model yields a consistent description of *p*- and *o*-benzosemiquinones, in contrast to previous models (see the introduction). The slopes of the regression lines defined by (1) and (2) are much steeper than the slope assumed by the original INDO parametrization, 539.86 G/ρ_{1s} [1]. In the investigation of monoprotonated **1** [11] a similarly steep slope was obtained, ~900 G/ρ_{1s}. The tendency to underestimate the hydrogen spin populations of semiquinones is probably an artifact of the INDO method.

The linear regression of the observed solvent sensitivities a'_H on the measured quantities ρ'_{1s} (see Table 1) is shown in Fig. 14. The least squares regression line is given by

$$a'_H = 241\ \rho'_{1s} + 0.11 \quad (3)$$

with regression coefficient 0.999 and standard deviation 0.18 G/X_{H_2O}. The observed results for **1** and **1a** are not strictly comparable to the results for **2**, **2a** and **2b** because different solvent mixtures were employed [6, 7]. Nevertheless, the correlation in Fig. 14 indicates that the INDO-ESF model is reasonably reliable for prediction of relative solvent sensitivities.

The results of the previously published EWMO investigation of **2**, **2a** and **2b** [7] are included in Table 1. The results are in all aspects consistent with the results obtained on the basis of the INDO method. The concordant results of the two different methods strongly indicate that the failure of previous methods to account for the spin distribution in these radicals is due to the neglect of the influence of the solvent.

4.3. 1,3-Benzosemiquinone **3**

This radical is essentially different from **1** and **2**. It is considerably less stable [25],

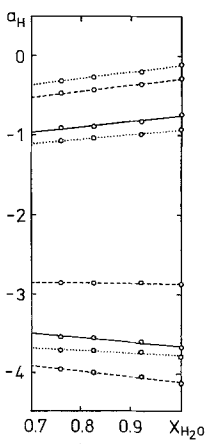

Fig. 12. Measured ring proton couplings a_H(G) of **2**, **2a** and **2b** as a function of the molar fraction of water X_{H_2O} in a H_2O-dioxane solvent mixture [7]. The symbolism is similar to Fig. 11

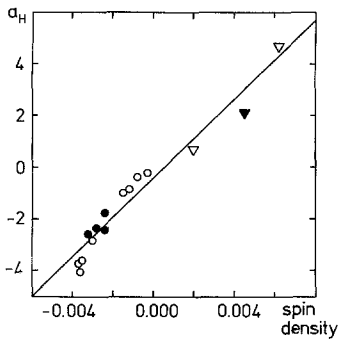

Fig. 13. Linear regression of the measured proton couplings a_H(G) of **1**, **1a**, **2**, **2a** and **2b** on the calculated H1*s* spin populations ($q = 1.1$e, see Table 1). Triangles indicate methyl protons; "solid points" indicate protons in **1** and **1a**

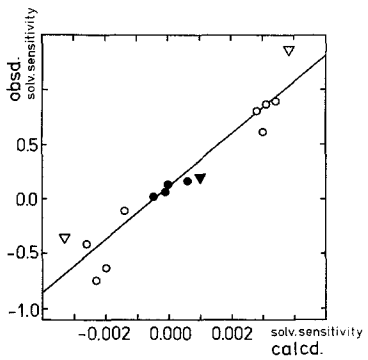

Fig. 14. Linear regression of the measured solvent sensitivities (G/X_{H_2O}) of the proton couplings of **1**, **1a**, **2**, **2a** and **2b** on the calculated sensitivities ($q = 1.1$e, see Table 1). The symbolism is similar to Fig. 13

and the spin distribution deviates markedly. In contrast to **1** and **2**, the major part of the spin density in **3** is not localized on the oxygen atoms but on the carbon

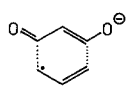

atoms at positions 4 and 6. **3** is probably best considered as a union of an allyl radical and a deprotonated malonic aldehyde. The calculated geometry is consistent with this point of view: the 1–6 and 3–4 bonds are essential single bonds (see Fig. 1). It appears from Fig. 15 that the ESF has no significant influence on the spin density in **3**; again, this is in marked contrast to the results for **1** and **2** (see Figs. 5 and 10). This is most likely a consequence of the localization of the spin density in the allyl fragment of **3** as indicated above. The predicted solvent dependencies of the hydrogen spin densities are very small, see Table 1. This result is in perfect agreement with the experimental evidence; the solvent sensitivities of the proton coupling constants of **3** are negligible [29].

5. Concluding Remarks

The most significant result of this investigation is the fact that a simple solvation

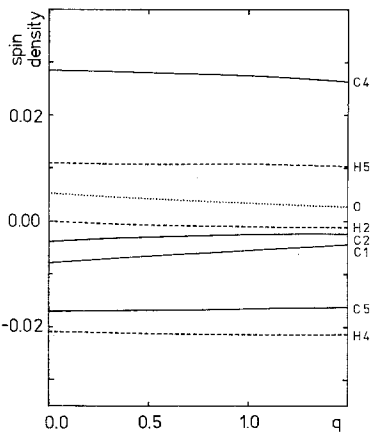

Fig. 15. Calculated 1*s* and 2*s* spin populations of **3** as a function of the ESF

model within the INDO framework leads to a consistent description of the proton splittings of 1,4- and 1,2-benzosemiquinones. Thus, no assumption needs to be made for one type of radical which is not made for the other. This result implies that the failure of traditional calculations to predict the relative proton coupling constants of these radicals is due to neglect of a large contribution from the solvent, particularly in the case of **2** and its derivatives [7]. Experimental investigation of the solvent dependence of the ^{13}C coupling constants of **2** would probably be quite rewarding as a check of the predictions for this radical (see Fig. 10).

Acknowledgement. The author is indebted to Dr. P. Bischof for the opportunity to use his MINDO/3-UHF computer program.

References

1. Pople, J. A., Beveridge, D. L., Dobosh, P. A.: J. Am. Chem. Soc. **90**, 4201 (1968); Pople, J. A., Beveridge, D. L.: Approximate molecular orbital theory. New York: McGraw-Hill 1970
2. Murrell, J. N., Harget, A. J.: Semi-empirical self-consistent-field molecular orbital theory of molecules. London: Wiley-Interscience 1972; Beveridge, D. L., in: Semiempirical methods of electronic structure calculations, Part B, Chapt. 5, Segal, G. A., ed. New York: Plenum Press 1977
3. Borg, D. C., in: Biological applications of electron spin resonance, Chapt. 7. Swartz, H. M., Bolton, J. R., Borg, D. C., eds. New York: Wiley 1972
4. Matsunaga, Y.: Bull. Chem. Soc. Jap. **33**, 1436 (1960); Wincow, G., Fraenkel, G. K.: J. Chem. Phys. **34**, 1333 (1961); Wincow, G.: J. Chem. Phys. **38**, 917 (1963); Kuboyama, A., Wada, K.: Bull. Chem. Soc. Jap. **38**, 1709 (1965); Kikuchi, O., Someno, K.: Bull. Chem. Soc. Jap. **40**, 2972 (1967); Silver, B. L.: Theoret. Chim. Acta (Berl.) **9**, 192 (1967); Edwards, T. G., Grinter, R.: Mol. Phys. **15**, 367 (1968)
5. Pilař, J.: J. Phys. Chem. **74**, 4029 (1970)
6. Spanget-Larsen, J., Pedersen, J. A.: J. Magn. Res. **18**, 383 (1975)
7. Pedersen, J. A., Spanget-Larsen, J.: Chem. Phys. Letters **35**, 41 (1975)
8. Schuster, P., Jakubetz, W., Marius, W.: Topics Current Chem. **60**, 1 (1975)

9. McCreery, J. H., Christoffersen, R. E., Hall, G. G.: J. Am. Chem. Soc. **98**, 7191 (1976); Miertuš, S., Kyseľ, O.: Chem. Phys. **21**, 27, 33, 47 (1977); and Refs. given in these papers
10. Spanget-Larsen, J.: Mol. Phys. **32**, 735 (1976)
11. Spanget-Larsen, J.: Chem. Phys. Letters **44**, 543 (1976)
12. Quantum Chemical Program Exchange, Indiana University: QCPE 141
13. Hales, B. J.: J. Am. Chem. Soc. **98**, 7350 (1976)
14. Stevenson, G. R., Alegria, A. E., Block, A. McB.: J. Am. Chem. Soc. **97**, 4859 (1975)
15. Bischof, P.: J. Am. Chem. Soc. **98**, 6844 (1976)
16. Bingham, R. C., Dewar, M. J. S., Lo, D. H.: J. Am. Chem. Soc. **97**, 1302 (1975)
17. Fairbourn, A., Lucken, E. A. C.: J. Chem. Soc. 258 (1963)
18. Pedersen, J. A.: Mol. Phys. **28**, 1031 (1974)
19. Loth, K., Graf, F., Günthard, Hs. H.: Chem. Phys. **13**, 95 (1976)
20. Loth, K., Graf, F., Günthard, Hs. H.: Chem. Phys. Letters **45**, 191 (1977)
21. Gendell, J., Freed, J., Fraenkel, G. K.: J. Chem. Phys. **37**, 2832 (1962)
22. Claxton, T. A., McWilliams, D.: Trans. Faraday Soc. **64**, 2593 (1968)
23. Stone, E. W., Maki, A. H.: J. Am. Chem. Soc. **87**, 454 (1965)
24. Gulick, W. M., Jr., Geske, D. H.: J. Am. Chem. Soc. **88**, 4119 (1966)
25. Pedersen, J. A.: J. Chem. Soc. Perkin II 424 (1973)
26. Linderberg, J., Öhrn, Y.: Propagators in quantum chemistry, p. 82. London: Academic Press 1973
27. Spanget-Larsen, J.: J. Electron Spectry. **2**, 33 (1973)
28. Adams, M., Blois, M. S., Jr., Sands, R. H.: J. Chem. Phys. **28**, 774 (1958)
29. Pedersen, J. A.: private communication

Received July 20, 1977